PHYSICAL REVIEW B **67**, 020508(R) (2003)

# Incommensurate anion potential effect on the electronic states of the organic superconductor (MDT-TSF) $(AuI_2)_{0.436}$

Tadashi Kawamoto and Takehiko Mori
*Department of Organic and Polymeric Materials, Graduate School of Science and Engineering, Tokyo Institute of Technology, O-okayama, Meguro-ku, Tokyo 152-8552, Japan*

Chieko Terakura, Taichi Terashima, and Shinya Uji
*National Institute for Materials Science, Tsukuba, Ibaraki 305-0003, Japan*

Kazuo Takimiya, Yoshio Aso, and Tetsuo Otsubo
*Department of Applied Chemistry, Graduate School of Engineering, Hiroshima University, Kagamiyama, Higashi-Hiroshima, Hiroshima 739-8527, Japan*

(Received 22 November 2002; published 21 January 2003)

Shubnikov–de Haas (SdH) oscillations have been investigated for the organic superconductor (methylenedithio-tetraselenafulvalene) $(AuI_2)_{0.436}$ with an incommensurate anion structure. Many SdH oscillations successively appear with increasing magnetic field, some of which are attributed to the Fermi surface reconstructed by the incommensurate anion potential. The reconstruction occurs neither by the fundamental anion periodicity $\boldsymbol{q}=0.436\boldsymbol{a}^*$ nor by $2\boldsymbol{q}$, but by $3\boldsymbol{q}$. The ''selection rule'' of the reconstructing vectors is associated with the magnitude of the incommensurate potential.

DOI: 10.1103/PhysRevB.67.020508 PACS number(s): 74.70.Kn, 71.18.+y, 71.20.Rv

In general, the energy-band calculation is impossible in the presence of an incommensurate periodic potential. Azbel first dealt with this problem within the generalized Kronig-Penny model, and pointed out that the incommensurate periodic potential is a natural intermediate between periodicity and randomness.[1] It creates a devil's-stair-type energy spectrum, and then one may expect fine structures in the quantum oscillations. For many years, the Fermi-surface (FS) topologies of metals and organic conductors have been studied using techniques such as the de Haas–van Alphen (dHvA) and Shubnikov–de Haas (SdH) oscillations.[2,3] It is generally believed that if an additional potential exists, the FS is reconstructed by the vector of this periodicity $\boldsymbol{q}$. The present paper, however, provides an unusual system where the FS reconstruction takes place not by the fundamental vector $\boldsymbol{q}$ but by the harmonics $3\boldsymbol{q}$ in an incommensurate crystal. Recently, Takimiya *et al.* have synthesized MDT-TSF (MDT-TSF: methylenedithio-tetraselenafulvalene depicted in Fig. 1), and have discovered superconductivity ($T_c=4.5$ K) in the $AuI_2$ salt.[4] We have found from the x-ray investigation that the anion lattice is incommensurate to the donor lattice, leading to such a nonstoichiometric composition as (MDT-TSF)$(AuI_2)_{0.436}$.[5] The present paper reports observation of SdH oscillations in (MDT-TSF)$(AuI_2)_{0.436}$.

Single crystals were prepared by the electrocrystallization reported in Ref. 4. For the SdH measurements, the samples were mounted in the dilution refrigerator in a 18-T superconducting magnet with one degree of rotational freedom with respect to the magnetic field, and the measurements were carried out by the four-probe method along the $a$ axis with ac current (usually 100 $\mu$A) down to 50 mK. Lock-in amplifiers and preamplifiers were used for the high-sensitive detection.

Figure 1 is the magnetic-field dependence of the electrical resistance at 50 mK ($B\|c$). Above 5 T magnetoresistance shows oscillating behavior. The oscillatory part (SdH signal) of the resistance is represented by $1-R(B)/R_0(B)$, subtracting the nonoscillatory background $R_0(B)$ [Fig. 2(a)]. Figure 2(b) shows the fast Fourier transformation (FFT) spectra obtained in field regions I–III defined in Fig. 2(a). In the low-field region (III) in Fig. 2(b), there are only two strong peaks $\alpha$ and $\beta$. Another orbit $\gamma$ appears clearly in the moderate field region (II). In the high-field region (I) the $\gamma$ orbit splits into $\gamma_1$ and $\gamma_2$, and another couple of high-frequency orbits $\delta_1$ and $\delta_2$ appear.

As shown in Fig. 3, the SdH frequencies show $1/\cos\theta$ behavior, indicating the cylindrical FS's, where $\theta$ is the angle between the magnetic field and the $c$ axis in the $bc$ plane.

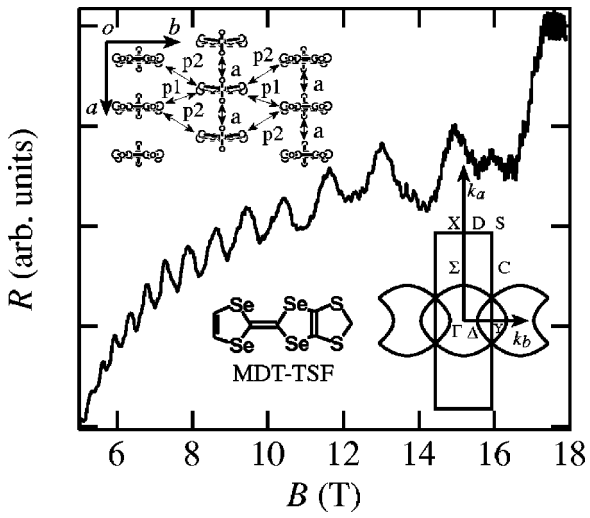


FIG. 1. Magnetoresistance of (MDT-TSF)$(AuI_2)_{0.436}$ at 50 mK ($B\|c$). Insets are the donor arrangement projected along the molecular long axis and the calculated FS without the incommensurate anion lattice potential (Ref. 6).

 

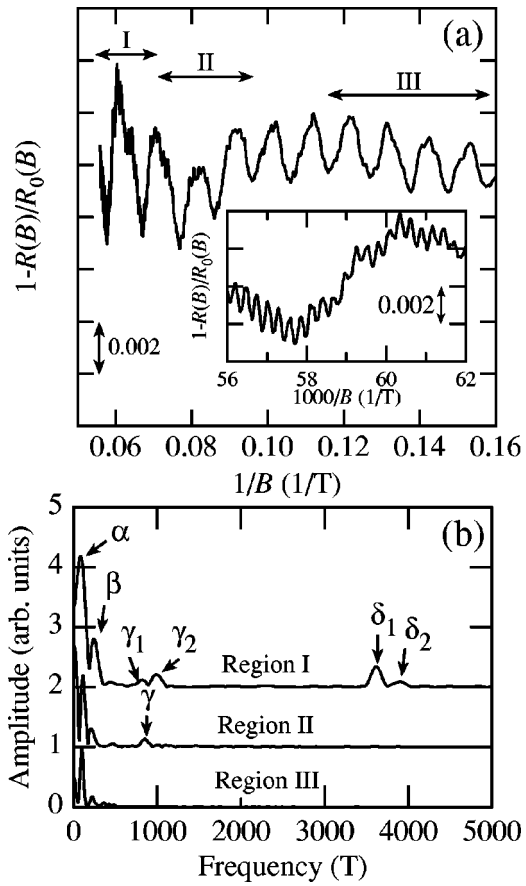


FIG. 2. (a) The SdH signal of the resistance $1-R(B)/R_0(B)$ for $B\|c$, where $R_0(B)$ is the nonoscillatory background. The inset is the high-field region. (b) The FFT spectra of the SdH oscillation in field regions I–III defined in (a).

The obtained frequencies are summarized in Table I with the ratios of the cross-sectional area to the first Brillouin zone (BZ) based on the donor lattice. The cyclotron radius of the $\delta_1$ orbit at 14 T is about 0.15 $\mu$m and is much longer than the Ginzburg-Landau (GL) coherence length at zero temperature, $\xi_a(0)\approx 260$ Å, extracted from the superconducting critical fields.[5] We can treat the present compound as a clean limit superconductor.

The SdH signals have been analyzed in the conventional way using the Lifshitz-Kosevich (LK) formula for the FFT amplitude

$$I_{FFT}\propto \sqrt{B}\,\frac{K\mu_c T/(B\cos\theta)}{\sinh[K\mu_c T/(B\cos\theta)]}\exp\left(\frac{-K\mu_c T_D}{B|\cos\theta|}\right)\times\left|\cos\left(\frac{\pi g\mu_b}{2\cos\theta}\right)\right|, \quad (1)$$

where $\mu_c$ is the effective cyclotron mass ratio $m^*/m_0$ at $\theta=0°$ ($m_0$ is the free electron mass), $T_D$ is the Dingle temperature, $g$ is the conducting electron $g$ factor, $\mu_b$ is the band mass ratio $m_b/m_0$ at $\theta=0°$, and $K=14.69$ T/K.[2]

Temperature dependences of the oscillation amplitudes divided by temperature, so-called mass plots, are presented in Fig. 4. The solid lines are the calculated results according to the LK formula. The determined effective cyclotron mass ratios are listed in Table I. The Dingle temperatures, simply determined from the field dependences of the oscillations, are also shown in Table I. The Dingle temperatures in Table I for $\gamma$ and $\delta$ approximately give the lower and upper limits, respectively, because the $\gamma$ and $\delta$ orbits are expected to include some Bragg reflection and magnetic breakdown points as discussed later.

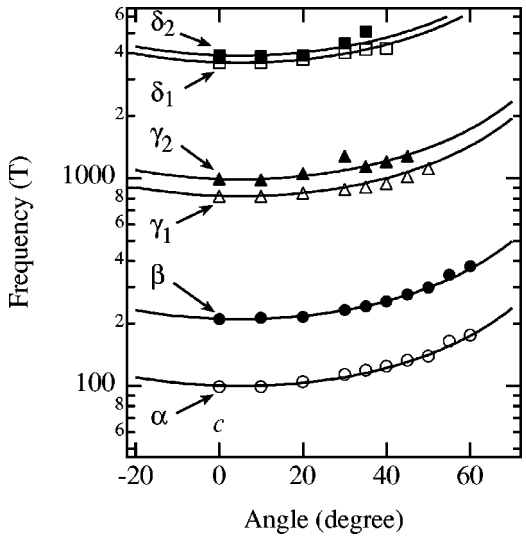


FIG. 3. Field angle dependence of the SdH frequencies. The solid lines show the $1/\cos\theta$ dependences.

The angular dependences of the oscillation amplitudes of both the $\alpha$ and $\beta$ orbits are shown in Fig. 5. The spin-splitting zero occurs at around $\theta\sim 55°$ for both orbits, showing that the $\beta$ orbit is not the second harmonic of the $\alpha$ orbit. Moreover, this enables the estimation of the product $g\mu_b$. From the LK theory, we can estimate $\mu_b\sim 0.8$ for the $\alpha$ orbit and 1.5 for the $\beta$ orbit at $\theta=0°$, where we assume $g=2.0$, independent of the field angle.

Our band calculation based on the donor arrangement has given overlapping cylindrical FS's (inset in Fig. 1), in which the cross section of the large cylinder is 43.6%, and the small overlapping area is about 8.5% of the first BZ.[6] This situa-

TABLE I. Shubnikov–de Haas frequencies, cross-sectional Fermi-surface-area ratios, cyclotron mass ratios, and the Dingle temperatures.

| Orbit | $F$(T) | $A_F/A_{BZ}$ (%) | $m^*/m_0$ | $T_D$ (K) |
|---|---|---|---|---|
| $\alpha$ | 100 | 1.2 | 0.6 | 0.1 |
| $\beta$ | 210 | 2.5 | 1.1 | 1.0 |
| $\gamma_1$ | 820 | 9.9 | [a] | [a] |
| $\gamma$ | 860 | 10.4 | 2.8 | 0.3 |
| $\gamma_2$ | 990 | 12.0 | [a] | [a] |
| $\delta_1$ | 3600 | 43.7 | 3.9 | 1.9 |
| $\delta_2$ | 3900 | 47.3 | 4.8 | 1.7 |

[a]The effective mass of the $\gamma$ orbit is the average of the $\gamma_1$ and $\gamma_2$ orbits, because we could not separate this in two peaks in some measurements.

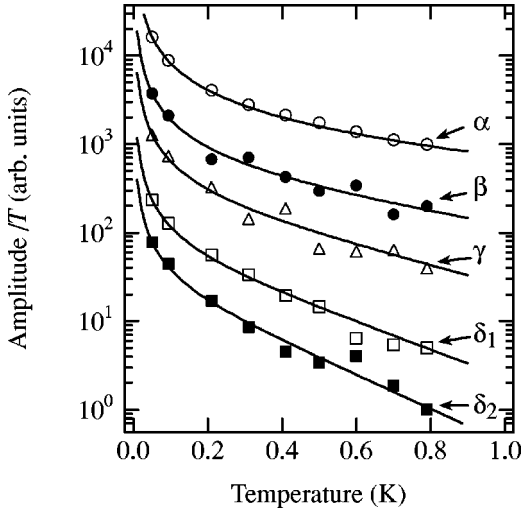


FIG. 4. Temperature dependences of the SdH oscillation amplitudes divided by temperature (mass plots). The solid lines are the fitted results.

tion resembles $\kappa$-$(ET)_2Cu(NCS)_2$ [ET, bis(ethylenedithio)tetrathiafulvalene], in which the overlapping area, corresponding to 18% of the first BZ, and the large FS area equal to the 100% first BZ have been observed in the SdH measurements.[8,9] The observed cross section of the $\delta_1$ orbit, $A_{F,\delta_1}/A_{BZ}=43.7\%$, is in agreement with the large cross section estimated from the band calculation (Fig. 6). This number is also equal to the amount of charge transfer coming from the anion content 0.436. The $\gamma$ orbit is assigned to the 8.5% overlapping area. Although the energy bands are degenerated on the C line owing to the donor lattice symmetry (*Pnma*), the incommensurate anion lattice along the *a* axis may destroy this symmetry. This broken symmetry makes the $\delta_1$ orbit a magnetic breakdown orbit that appears only at high fields, similarly to the 100% orbit in $\kappa$-$(ET)_2Cu(NCS)_2$.

In Fig. 2(b), two close SdH frequencies tend to appear as pairs, $\delta_1$-$\delta_2$ and $\gamma_1$-$\gamma_2$. When the two SdH frequencies arising from the maximum and minimum cross-sectional areas

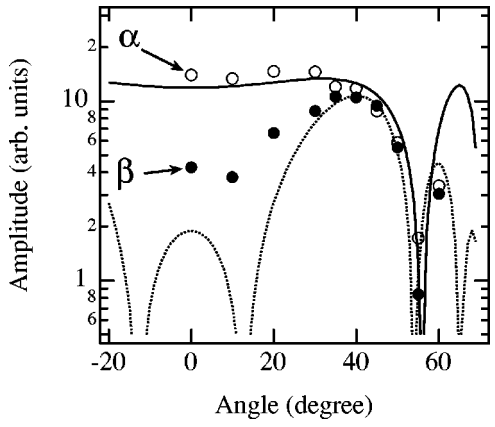


FIG. 5. Field angle dependence of the SdH oscillation amplitudes of the $\alpha$ and $\beta$ orbits. The solid and dotted lines are the fitted results.

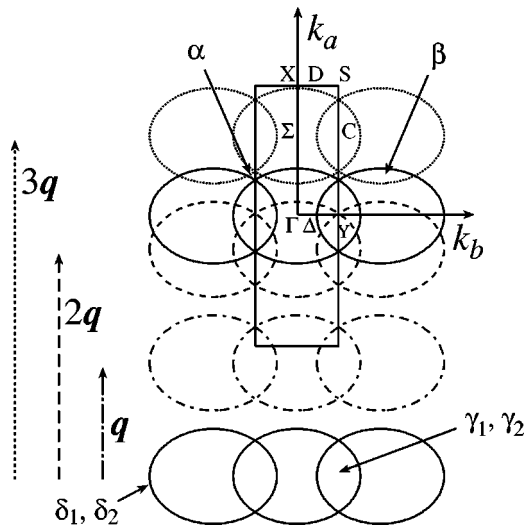


FIG. 6. Reconstructed FS in the $a^*b^*$ plane translated by $\boldsymbol{q}$ (dash-dotted lines), $2\boldsymbol{q}$ (dashed lines), and $3\boldsymbol{q}$ (dotted lines) on to the original FS (solid lines). The first Brillouin zone is calculated from the donor lattice.

of the FS are $f_1$ and $f_2$, respectively, the ratio is given by $2t_z/\overline{E_F}=(f_1-f_2)/(f_1+f_2)$. Here $t_z$ is the interlayer transfer integral and $\overline{E_F}$ is the averaged Fermi energy. If we assume a parabolic energy band, the Fermi energy is written as $\overline{E_F}=\hbar^2\overline{k_F^2}/2\overline{m}^*=\hbar^2\overline{A_F}/2\pi\overline{m}^*$, where $\overline{A_F}$ is the averaged value of the cross sections of the FS and $\overline{m}^*$ is the averaged cyclotron mass. From the set of the $\delta_1$ and $\delta_2$ orbits, we obtain $t_z\sim 2$ meV. The set of the $\gamma_1$ and $\gamma_2$ gives the same value, 2 meV. These interlayer transfer integrals are much larger than that of $\kappa$-$(ET)_2Cu(NCS)_2$ (0.04 meV).[10] This is consistent with the long GL coherence length, $\xi_c(0)\approx 50$ Å.[5]

Two low-frequency orbits, the $\alpha$ and $\beta$ orbits, are not explained from the band calculation. This indicates that the FS is reconstructed by the incommensurate anion potential. Among inorganic compounds, $Hg_{3-\delta}AsF_6$ and $Hg_{3-\delta}SbF_6$ are known as systems with incommensurate mercury chains, and the dHvA frequencies consisting of six kinds of cylindrical orbits have been observed.[11] The FS's of these inorganic compounds are reconstructed by the fundamental incommensurate mercury-chain periodicity, $\boldsymbol{q}=a^*(\delta,\pm\delta,0)$. In $(MDT\text{-}TSF)(AuI_2)_{0.436}$, the incommensurate potential of the anion lattice with $\boldsymbol{q}=0.436\boldsymbol{a}^*$ reconstructs the FS as shown in Fig. 6, where we assume the FS shape to be an ellipsoid with the overlapping area corresponding to the $\gamma_1$ orbit. Although the vector $\boldsymbol{q}$ does not make a new pocket, $2\boldsymbol{q}$ and $3\boldsymbol{q}$ lead to new overlapping regions.

The $3\boldsymbol{q}$ vector makes two new pockets, which are about 3% and 0.3% of the first BZ. The former is assigned to the $\beta$ orbit. Although the latter pocket does not exactly agree with the $\alpha$ orbit, a small pocket is considered to be sensitive to the reconstruction. Therefore the $\alpha$ orbit can be assigned to this smallest pocket. The $2\boldsymbol{q}$ vector makes a new overlapping area of 25%, but this is too large to be interpreted as the observed $\alpha$ and $\beta$ frequencies. Then the observed orbits are explained by the $3\boldsymbol{q}$ reconstruction of the FS.

In contrast to the mercury chain compounds explained by a simple $\boldsymbol{q}$ vector originating in the incommensurate mercury chain, the FS of the present compound is reconstructed by $3\boldsymbol{q}$. This characteristic reconstruction is related to the intensity of the anion sublattice reflections observed in the x-ray oscillation photograph.[5] Although the spots of both $\boldsymbol{q}$ and $3\boldsymbol{q}$ are clearly observed, the $2\boldsymbol{q}$ spot is not found in the x-ray photograph. This is associated with the absence of the $2\boldsymbol{q}$ reconstruction. The x-ray $3\boldsymbol{q}$ intensities are even stronger than the $\boldsymbol{q}$ intensities. The $\boldsymbol{q}$ vector comes from the fundamental repeating period of the $AuI_2$ anion (9.221 Å), while the $3\boldsymbol{q}$ potential is strong because this is associated with the average distance of Au-I and I-I (3.040 Å). This structural feature also explains the absence of the $2\boldsymbol{q}$ reflections. The conduction electrons mainly feel the periodic potential generated by the interatomic distance of the $AuI_2$ chain.

The successive appearance of many SdH oscillations in (MDT-TSF)$(AuI_2)_{0.436}$ reminds us of Azbel's prediction.[1] In the real materials, however, the magnitudes of various sublattice potentials are different, and only one or a few modulations are usually predominant. This suppresses the appearance of the fine structure in the quantum oscillations and affords the ''selection rule'' of the reconstructing vectors. The present system provides a very rare case in which the principal potential is not of the fundamental periodicity.

In summary, (MDT-TSF)$(AuI_2)_{0.436}$ has four kinds of corrugated cylindrical FS's demonstrated by the SdH oscillations. The two large orbits are explained from the donor arrangement, in agreement with the charge transfer estimated from the x-ray investigation. Two medium orbits are consistent with the overlapping area of the large FS. The other two orbits originate in the incommensurate anion potential. The observation of the SdH oscillations shows that the incommensurate anion potential works as a weak periodic potential for the conduction electrons on the MDT-TSF molecules rather than a random potential. The characteristic reconstructing vector depends on the magnitude of the incommensurate potential; this works as the ''selection rule'' of the reconstructing vectors. The present quantum oscillation measurement is, to the best of our knowledge, the first detection of the incommensurate anion lattice effect on the FS in organic conductors.

This work was partially supported by a Grant in Aid for Scientific Research (Grant No. 14740377) from the Ministry of Education, Science, Sports and Culture.

[1] M.Ya. Azbel, Phys. Rev. Lett. **43**, 1954 (1979).

[2] D. Shoenberg, *Magnetic Oscillations in Metals* (Cambridge University Press, Cambridge, 1984).

[3] T. Ishiguro, K. Yamaji, and G. Saito, *Organic Superconductors*, 2nd ed. (Springer, Berlin, 1998).

[4] K. Takimiya *et al.*, Angew. Chem. Int. Ed. **40**, 1122 (2001).

[5] T. Kawamoto *et al.*, Phys. Rev. B **65**, 140508(R) (2002).

[6] This is different from our previous band calculation in Ref. 5, because $3d$ orbitals of S and $4d$ orbitals of Se are not included. This reduces the transverse interactions, resulting in elliptical FS. This anisotropic shape is consistent with the anisotropic optical reflectance spectra in the $ab$ plane (Ref. 7).

[7] T. Kawamoto *et al.* (unpublished).

[8] K. Oshima *et al.*, Phys. Rev. B **38**, 938 (1988).

[9] T. Sasaki, H. Sato, and N. Toyota, Solid State Commun. **76**, 507 (1990).

[10] J. Singleton *et al.*, Phys. Rev. Lett. **88**, 037001 (2002).

[11] E. Batalla, F.S. Razavi, and W.R. Datars, Phys. Rev. B **25**, 2109 (1982).